N^* electroproduction and propagation in nuclei

L. B. Weinstein,[a] J. Morrison, A. Perry,[b] H. Baghaei,[c] W. Bertozzi, W. U. Boeglin,[d]
J. M. Finn,[e] J. Glickman,[f] C. E. Hyde-Wright,[g] N. Kalantar-Nayestanaki,[h] R. W. Lourie,[c] J. A. Nelson,[i]
S. Penn, W. W. Sapp, C. P. Sargent, and P. E. Ulmer[j]
Department of Physics, Massachusetts Institute of Technology, Cambridge, Massachusetts 02139

B. H. Cottman,[k] L. Ghedira, and E. J. Winhold
Department of Physics, Rensselaer Polytechnic Institute, Troy, New York 12181

J. R. Calarco and J. Wise[l]
Department of Physics, University of New Hampshire, Durham, New Hampshire 03824

P. Boberg,[m] C. C. Chang, N. S. Chant, P. G. Roos, and D. Chang[n]
Department of Physics and Astronomy, University of Maryland, College Park, Maryland 20742

K. Aniol, M. B. Epstein, and D. J. Margaziotis
Department of Physics and Astronomy, California State University, Los Angeles, California 90032

C. Perdrisat and V. Punjabi
Department of Physics, College of William and Mary, Williamsburg, Virginia 23185

R. Whitney
Continuous Electron Beam Accelerator Facility, Newport News, Virginia 23606
(Received 10 August 1992)

We have measured the $^{12}C(\gamma^*,\pi^-p)^{11}C_{g.s.}$ cross section using virtual bremsstrahlung at three points at invariant masses of 1444 and 1530 MeV. At low neutron initial momentum ($p_m \approx 60$ MeV/c) and large N^* momentum ($p_{N^*} \approx 750$ MeV/c) the measured cross section is at or below the distorted wave impulse approximation (DWIA) calculation. At larger initial momentum ($p_m \approx 220$ MeV/c) and smaller N^* momentum ($p_{N^*} \approx 500$ MeV/c), the measured cross section is almost twice as large as the DWIA calculation. This discrepancy might be due to N^*-nucleus interactions.

PACS number(s): 25.20.Lj, 13.60.Rj

I. INTRODUCTION

In this paper, we report a measurement of the (γ^*,π^-p) reaction in the second resonance region ($W \approx 1530$ MeV) and its variation with invariant mass and recoil momentum. This measurement provides the first information on N^* electroproduction and propagation in nuclei.

The study of Δ and N^*-nucleus interactions provides information on the role of baryon internal structure in the strong interaction [1]. There has been a great deal of study of the $\Delta(1232)$ resonance in nuclei, primarily using

[a]Present address: Department of Physics, Old Dominion University, Norfolk, VA 23529.
[b]Present address: Department of Physics, Rensselaer Polytechnic Institute, Troy, NY 12181.
[c]Present address: Department of Physics, University of Virginia, Charlottesville, VA 22901.
[d]Present address: Institut fur Kernphysik, Der Universitat Mainz, 6500 Mainz 1, Germany.
[e]Present address: Department of Physics, College of William and Mary, Williamsburg, VA 23185.
[f]Present address: 9308 Cheney Hill Rd., College Park, MD 20740.
[g]Present address: Department of Physics, University of Washington, Seattle, WA 98195.
[h]Present address: Department of Physics and Astronomy, Free University, 1081 HV Amsterdam, The Netherlands.
[i]Present address: 53 Bridge St., Beverly, MA 01915.
[j]Present address: Continuous Electron Beam Accelerator Facility, Newport News, VA 23606.
[k]Present address: I-Kinetics, Inc., 19 Bishop Allen Drive, Cambridge, MA 02139.
[l]Present address: Department of Physics, University of Colorado, Boulder, CO 80306.
[m]Present address: Code 4154, Naval Research Laboratory, Washington, DC 20375.
[n]Present address: Shell Western Division, P.O. Box 576, Houston, TX 77001.

 ©1993 The American Physical Society

the (π,π'), $(\pi,\pi'p)$, and (γ,π) reactions, with some (γ,π^-p) measurements. Calculations involving the Δ-hole model, that describe the resonance propagation and decay in the nucleus, typically describe the data much better than distorted-wave impulse approximation (DWIA) calculations which only include the production cross section and the initial and final-state interactions. For example, the Δ-hole model describes the 240 MeV $^{16}O(\pi^{\pm},\pi^{\pm}p)$ data of Kyle *et al.*, [2] much better than DWIA. Similarly, the Δ-hole model calculation of Koch and Moniz [3] describes the 290 MeV $^4He(\gamma,\pi^0)$ data of Tieger *et al.* [4] while the DWIA calculation of Girija *et al.* [5] underestimates the data by 30%.

II. THIS MEASUREMENT

We performed the experiment at the Massachusetts Institute of Technology Bates Linear Accelerator Center using the magnetic spectrometers MEPS and OHIPS to detect pions and protons, respectively. MEPS is a quadrupole-quadrupole-split dipole vertical bend spectrometer with $\Delta p/p=20\%$, $\Delta\Omega=20$ msr and momentum resolution $\delta p/p=10^{-3}$ [6]. OHIPS is a quadrupole-quadrupole-dipole vertical bend spectrometer with $\Delta p/p=10\%$, $\Delta\Omega=5$ msr, and $\delta p/p=10^{-3}$ [7]. Each spectrometer was instrumented with a two-plane vertical drift chamber to measure the particle coordinates (x,y,θ,ϕ) and a scintillator array for trigger definition. The pion spectrometer was also equipped with an aerogel $(n=1.05)$ Čerenkov counter for off-line electron-pion separation. We used electron beams of approximately 700 and 800 MeV incident on a 200 mg/cm^2 natural carbon target. We did not use a radiator. We measured the virtual (γ^*,π^-p) cross section at three points, shown in Table I. For each data point we fixed the pion spectrometer and scanned the magnetic field of the proton spectrometer to measure the cross section over a range of missing energies. We acquired these data simultaneously with $^{12}C(e,e'p)$ data [8,9].

We calibrated the solid angles and efficiencies of the spectrometers singly and in coincidence using the $^1H(e,e')$, $^{12}C(e,e')$, and $^1H(e,e'p)$ reactions. The systematic uncertainties of 7% for each point are due primarily to uncertainty in the beam energies and to statistical uncertainty in the calibration measurements. The missing energy resolution (FWHM) was ≈2.5 MeV, consistent with the 3×10^{-3} energy spread of the beam. For each point we sampled the accidental coincidence background and subtracted it from the real coincidence missing energy spectrum. The signal-to-noise ratio varied from 1:4 to 1:1.

TABLE I. (γ^*,π^-p) kinematics. The first four columns show the incident electron beam energy (the photon end-point energy), the pion central momentum, the pion laboratory angle, and the proton laboratory angle. The last four columns contain calculated quantities. They show the invariant mass W of the $(p\pi^-)$ system, the missing momentum p_m (which in the spectator model is equal and opposite to the initial neutron momentum in the nucleus), the N^* momentum in the nucleus p_{N^*} ($p\pi^-$ total momentum), and the angle of the π^- relative to the N^* laboratory momentum direction in the center-of-mass frame. These quantities are averaged over the experimental acceptances for the reaction $^{12}C(\gamma^*,\pi^-p)^{11}C_{g.s.}$.

	E_e MeV	p_π MeV/c	θ_π deg	θ_p deg	W MeV/c^2	p_m MeV/c	p_{N^*} MeV/c	$\theta^{\pi}_{c.m.}$ deg
A	698	343	90.0	27.9	1444	67	728	134
B	796	331	118.1	17.0	1526	56	780	152
C	696	380	129.7	17.0	1537	222	494	159

We calculated various kinematic quantities using the photon end-point energy E_e, the ground-state missing energy, and the proton and pion angles and momenta and integrating over the experimental acceptances. These are shown in Table I.

Although the kinematics were chosen for the $^{12}C(e,e'p)$ measurements, they also provide systematic $^{12}C(\gamma^*,\pi^-p)$ data. There are two points at almost the same invariant mass ($W\approx1530$ MeV/c^2) on top of the $S_{11}(1535)$, $I(J^P)=\frac{1}{2}(\frac{1}{2}^-)$, and $D_{13}(1520)$, $I(J^P)=\frac{1}{2}(\frac{3}{2}^-)$, resonances but with different recoil momentum and there are two points at almost the same recoil momentum ($p_m\approx60$ MeV/c) but different invariant mass.

We measured the (γ^*,π^-p) cross section as a function of the missing energy, $\varepsilon_m=E_e-T_p-E_\pi$. ε_m equals the removal energy of the struck nucleon (18.5 MeV) plus the kinetic energy of the recoiling $A-1$ system plus the excitation energy of the $A-1$ system, $E_{\rm excit}$. Figure 1 shows the first 40 MeV of the measured cross section. These spectra are the convolution of the virtual bremsstrahlung spectrum with the nuclear excitation spectrum. (Note that we expect the end point of the cross section to be at $\varepsilon_m=18.5$ MeV $+T_{A-1}\pm\delta E_e$, where δE_e is the uncertainty in the incident energy and T_{A-1} is approximately 2.5 MeV for point C and 0.5 MeV for points A and B.)

We determined the $^{12}C(\gamma^*,\pi^-p)^{11}C_{g.s}$ cross section in the following manner: Since, in $^{12}C(e,e'p)$, $1p_{3/2}$ proton knockout to the ground state of ^{11}B dominates the cross section for the first 10 MeV of excitation energy [10], we assume that, in $^{12}C(\gamma^*,\pi^-p)$, $1p_{3/2}$ neutron knockout to the ground state of ^{11}C also dominates the cross section for the first 10 MeV of missing energy. We also assume that the (γ^*,π^-p) cross section does not vary over 10 MeV of photon energy.

The observed cross section is now (valid only in the first 10 MeV below the end point)

$$\frac{d^4\sigma(\varepsilon_m=E_e-E_\gamma)}{d\Omega_p d\Omega_\pi dE_\pi d\varepsilon_m}=N_\gamma(E_e,E_\gamma)\sigma_{g.s.}\frac{1}{E_\gamma}\ , \tag{1}$$

where

$$\sigma_{g.s.}=\left.\frac{d^3\sigma(E_{\rm excit}=0)}{d\Omega_p d\Omega_\pi dE_\pi}\right|_{E_\gamma=E_e}\ , \tag{2}$$

where $N_\gamma(E_e,E_\gamma)$ is the energy weighted number of virtual photons of energy E_γ per incident electron (of energy E_e),

$$\frac{d^4\sigma(\varepsilon_m=E_e-E_\gamma)}{d\Omega_p d\Omega_\pi dE_\pi d\varepsilon_m}$$

is the measured (γ^*,π^-p) cross section, and

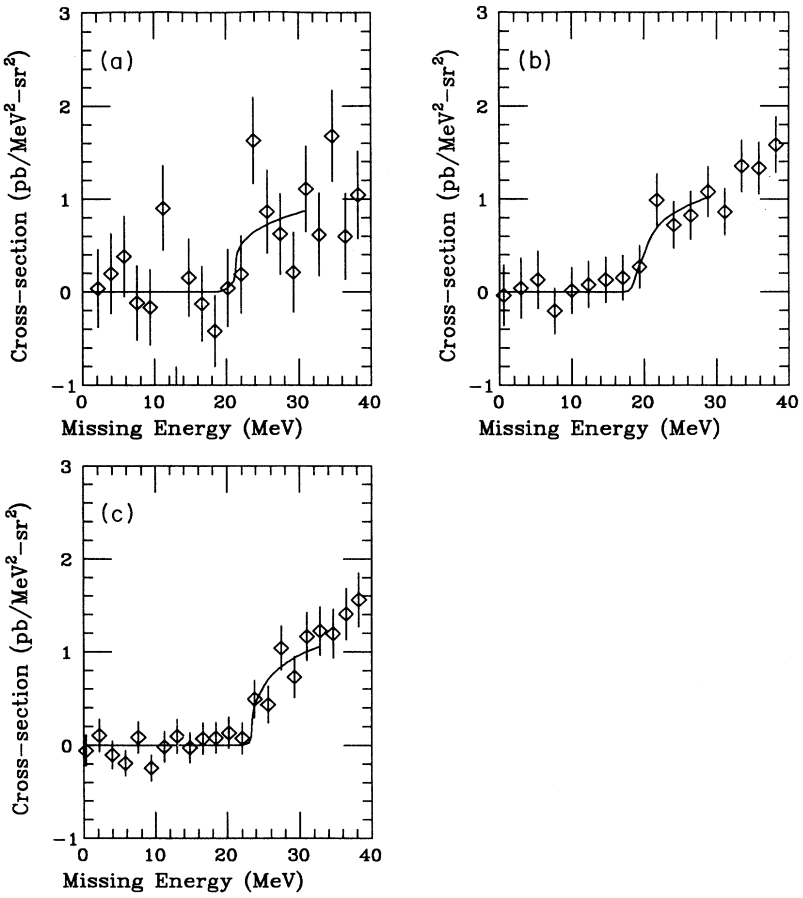

FIG. 1. Bremsstrahlung fit to (γ^*,π^-p) cross sections. The points are the $^{12}C(\gamma^*,\pi^-p)$ cross sections and the solid lines are the fits to the data for the $^{12}C(\gamma,\pi^-p)^{11}C_{g.s.}$ transition. Only the first 10 MeV of data beyond the end point was used for each fit. (a) data set A, (b) data set B, (c) data set C.

$$\left.\frac{d^3\sigma(E_{\text{excit}}=0)}{d\Omega_p d\Omega_\pi dE_\pi}\right|_{E_\gamma=E_e}$$

is the $^{12}C(\gamma^*,\pi^-p)^{11}C_{g.s.}$ ground-state transition cross section that we want to determine. This technique of fitting a virtual bremsstrahlung spectrum to experimental data in order to extract a ground-state cross section has been tested and works well [11–13].

Virtual bremsstrahlung dominated the photon yield. Virtual bremsstrahlung is equivalent to $\approx 2\%$ of a radiation length. Real bremsstrahlung without a separate radiator can be approximated by radiation in the first part of the target followed by a photon-nucleus interaction in the remainder. Thus the ratio of real to virtual bremsstrahlung is

$$\frac{1}{0.02t}\int_0^1 (xt/L)(1-x)t\,dx\ ,$$

where t is the target thickness (200 mg/cm^2), L is the radiation length of carbon (40 gm/cm^2), and x is the fraction of the target in which the real bremsstrahlung occurs. Real bremsstrahlung is thus 4% of virtual bremsstrahlung.

We used the virtual bremsstrahlung spectrum of Tiator and Wright [14] simplified for infinitely massive recoil and multiplied by 1.04 to account for the small amount of real bremsstrahlung:

$$N_\gamma(E_e,E_\gamma)=\frac{\alpha E_\gamma^2}{2\pi E_e^2}\left[\left[1-\frac{2a}{E_\gamma^2}\right]\ln\left[\frac{a-b}{a+b}-\frac{4b}{E_\gamma^2}\right]\right], \quad (3)$$

where $b=E_e(E_e-E_\gamma)$ and $a=m_e^2-b$. Using N_γ, we fitted the $^{12}C(\gamma^*,\pi^-p)^{11}C_{g.s.}$ cross section $\sigma_{g.s.}$ and the photon end-point energy E_e to the first 10 MeV of the data beyond the end point. The fitted endpoint energies are within the uncertainty of the experimentally determined beam energy, indicating the validity of the fitting procedure. The fits are shown in Fig. 1.

We corrected the observed cross sections for the effect of pion decay in the spectrometer. We used correction factors of 1.30 (data set A), 1.31 (data set B), and 1.27 (data set C). The $^{12}C(\gamma^*,\pi^-p)^{11}C_{g.s.}$ cross sections are shown in column 2 of Table II.

TABLE II. $^{12}C(\gamma^*,\pi^-p)^{11}C_{g.s.}$ cross sections. The first uncertainty includes statistical and fitting effects, the second uncertainty is systematic. Both uncertainties are included in quadrature in the ratio of data to DWIA. Model uncertainties are not included.

	Cross Section (nb/MeV sr^2)			
	data	PWIA	DWIA	data/DWIA
A	81±19±6	297	138	0.59±0.15
B	121±19±8	258	135	0.90±0.15
C	108±13±8	110	57	1.90±0.27

III. THEORY CALCULATIONS

There are three interconnected processes that can be included in theories of the (γ^*,π^-p) reaction: (1) the production cross section, which is usually taken from a fit to the elementary cross section, (2) the propagation and decay of the resonance in the nucleus. In the case of the $\Delta(1232)$, this is described via the Δ-hole model, and (3) the initial-and-final-state interactions of the hadrons involved, which are usually described using an optical potential. Ideally, we would use a model which contains all of these processes. Since we do not currently have any information on the propagation and decay of the N^* in the nucleus, we will have to infer that information from differences between the observed cross sections and DWIA calculations, which only include the production cross section and the final-state interactions of the outgoing hadrons.

We calculated the factorized DWIA cross section using a modified version of the code THREEDEE. [15] The DWIA (γ^*,π^-p) formalism is also derived by Laget [16]:

$$\left.\frac{d^4\sigma}{d\Omega_p d\Omega_\pi dE_\pi d\varepsilon_m}\right|_{(\gamma^*,\pi^-p)} = K\sigma^{\rm cm}_{\gamma n\to\pi^-p} S^D(p_m,E_{\rm excit},p_p)\ , \quad (4)$$

where K is a kinematical factor and $\sigma^{\rm cm}_{\gamma n\to\pi^-p}$ is the elementary pion production cross section in the center of mass of the γn system. $S^D(p_m,E_{\rm excit},p_p)$ is the distorted spectral function:

$$S^D(p_m,E_{\rm excit},p_p)=\sum_\alpha |\Phi^D_\alpha(p_m,p_p)|^2 S_\alpha \delta(E_{\rm excit}-E_\alpha)\ , \quad (5)$$

where S_α is the spectroscopic factor for state α, E_α is the excitation energy of state α, and Φ^D_α is the overlap integral between the initial neutron wave function and the distorted wave functions of the outgoing particles:

$$\Phi^D_\alpha=\int \chi^{-(*)}_{\pi^-}\chi^{-(*)}_p e^{i\mathbf{k}_\gamma\cdot\mathbf{r}}\phi_\alpha(\mathbf{r})d\mathbf{r}\ . \quad (6)$$

$\chi^{-(*)}$ is an outgoing distorted wave, $e^{i\mathbf{k}_\gamma\cdot\mathbf{r}}$ is the photon operator, and $\phi_\alpha(\mathbf{r})$ is the bound-state wave function for state α. In the absence of distortions, S^D reduces to the probability of finding a neutron in the nucleus with initial momentum $-p_m$ and whose removal would leave the nucleus with excitation energy $E_{\rm excit}$.

We used the measured elementary $\gamma n\to\pi^-p$ cross sections, $\sigma^{\rm cm}_{\gamma n\to\pi^-p}$, and target analyzing powers as parametrized by Arai and Fujii. [17] The latter was necessary to account for the effective struck nucleon polarization which is a result of the spacial localization of the reaction in conjunction with the spin-orbit part of the potential in which the nucleon is bound. This effective polarization is easily calculated in the DWIA. In $(p,2p)$ reactions it is known as the Maris effect. The measured elementary cross sections automatically include both resonant and nonresonant parts. We only used the free cross sections; we made no corrections for off-shell effects or dynamical medium modifications.

We generated the neutron p-shell momentum distribution from $\phi(r)$, a coordinate space wave function calculated using a Woods-Saxon proton potential with the rms radius fit to ^{12}C$(e,e'p)$ data with the neutron binding energy [10][18]. We used the proton optical potential of Nadasen *et al.* [19] and the pion optical potential of Cottingame and Holtkamp [20] to describe the final state distortions of the proton and pion respectively, $\chi_p^{-(*)}$ and $\chi_{\pi^-}^{-(*)}$. We used a spectroscopic factor S_{p_1} of 2.5, consistent with proton spectroscopic factors from ^{12}C$(e,e'p)$ [8][10]. We integrated the plane-wave impulse approximation (PWIA) and DWIA cross sections over the experimental acceptances.

Table II shows the results. The PWIA cross section does not include the effects of final-state interactions (FSI). The DWIA includes distortions of the π^- and proton waves in the nucleus, but does not include any interaction of the intermediate N^* resonance with the nucleus. The final-state interactions reduce the impulse approximation cross section by a factor of approximately 2. Cross sections shown do not include model uncertainties.

In order to study the sensitivity of the calculation to the neutron bound-state wave function, we generated a different neutron p-shell momentum distribution from a coordinate space wave function calculated using the Elton-Swift proton potential [21]. The rms radius of this $1p_{3/2}$ wave function was 2.62 fm compared to 2.76 fm for the Woods-Saxon bound-state wave-function fit to ^{12}C$(e,e'p)$ data. This momentum distribution decreased the DWIA calculation for data sets A and B by about 20%, increasing the data/DWIA ratios to about 0.7 and 1.1, respectively. It left the cross section calculated for data set C unchanged.

We also examined the effects using different prescriptions for the off-shell kinematics. We used the average of the final-energy prescription and the initial energy prescription. The largest effect was in data set C which was the farthest off-shell (had the largest recoil momentum). Had we used only the initial energy prescription, the ratios for data sets A, B, and C would have been 0.58, 0.97, and 2.27, respectively.

We expect that different optical potentials can change the DWIA calculation by $\approx$20%. At these proton energies, ^{12}C$(e,e'p)$ DWIA cross sections calculated with different optical potentials vary by $\approx$10% [22]. Pham *et al.* found that their calculated cross sections for ^{16}O(γ,π^-p) varied by 20% with different optical potentials [23]. Pham's data were taken at significantly lower proton and pion energies where final-state distortions are larger.

There is an additional uncertainty in the treatment of the final-state interaction due to the outgoing pion. Since we only measured pions emitted at backward angles, the pions' energies are reduced from the value they would have for decay of a free N^*. The pion kinetic energies are approximately 220–270 MeV, which are on the tail of the $\Delta(1232)$. Thus we might need to use the Δ-hole model to describe the final-state interaction of the outgoing pions. Data set C at T_π=270 MeV will be less sensitive to these effects than data sets A or B. We expect that the total model uncertainty from the choice of wave function, off-shell kinematical prescription, and optical potential is 20%–30%.

The DWIA calculation is within a factor of two of the data. If we neglect model uncertainties, then the measured cross section is $\approx 2.5\sigma$ below the calculation for data set A, less than 1σ below the calculation for data set B, and $\approx 3.5\sigma$ above the calculation for data set C. If we include model uncertainties, then the discrepancies for data sets A and C are less significant.

IV. DISCUSSION AND CONCLUSION

We have measured the $^{12}C(\gamma^*,\pi^- p)$ cross section at three different kinematic points at invariant masses of 1444 and 1530 MeV. Below the S_{11} and D_{13} resonances at $W=1444$ MeV, at low neutron initial momentum ($p_m \approx 60$ MeV/c) and large N^* momentum ($p_{N^*} \approx 750$ MeV/c) the DWIA calculation is larger than the measured cross section. At the resonances ($W=1530$ MeV), at low neutron initial momentum ($p_m \approx 60$ MeV/c) and large N^* momentum ($p_{N^*} \approx 750$ MeV/c) the DWIA calculation is equal to the measured cross section. As mentioned above, these two low initial neutron momentum points are sensitive to the neutron bound-state wave function. At the resonances ($W=1530$ MeV), at larger initial momentum ($p_m \approx 220$ MeV/c) and smaller N^* momentum ($p_{N^*} \approx 500$ MeV/c) the DWIA calculation is only half of the measured cross section.

This difference between measured cross section and DWIA calculation might be due to either an incorrect nucleon bound-state wave function or the effects of N^*-nucleus interactions. Since, in $(e,e'p)$, recoil momenta of 50 and 200 MeV/c are equally well described by DWIA calculations [10], the nucleon wave function should be as good at 200 as at 50 MeV/c. Also, data set C, at $p_m \approx 220$ MeV/c, is not very sensitive to the bound-state wave function. It is expected that, at smaller N^* momenta in the nucleus, the N^*-nucleus interaction should be larger. [24] Thus, this difference between measurement and DWIA at the smaller N^* momentum could be due to N^* propagation in the nucleus.

These results are different from previous $(\gamma,\pi^- p)$ measurements. There are two previous measurements of the $(\gamma,\pi^- p)$ reaction in complex nuclei that specified the nuclear final state, all at the $\Delta(1232)$ [23–27]. See van der Steenhoven [28] for a review of recent experiments.

Glavanakov and collaborators at Tomsk measured $^{12}C(\gamma,\pi^- p)$ at the $\Delta(1232)$ using real bremsstrahlung at a backward pion angle. They calculated the DWIA cross section using the eikonal approximation for the distorted waves. While the eikonal approximation is not as good as a full partial-wave analysis, the calculation described their data well.

Pham *et al.* measured the $^{16}O(\gamma,\pi^- p)^{15}O_{g.s.}$ cross section at the $\Delta(1232)$. They measured the proton angular distribution around quasifree $\Delta(1232)$ production kinematics for two different pion angles, 64° and 120°, using the real-photon bremsstrahlung end point. The $\Delta(1232)$ momentum in the nucleus was approximately 430 MeV/c at $\theta_\pi=120°$ and was approximately 310 MeV/c at $\theta_\pi=64°$. The angular distribution of the outgoing protons was consistent with the neutron initial momentum distribution, i.e.: with a quasifree knockout process. They calculated the DWIA cross section using a modified version of the code THREEDEE. They assumed that there were 3.6 p-shell neutrons in ^{16}O, consistent with the spectroscopic factors measured in $(e,e'p)$. The ratio of data to theory was ≈ 1 for $\theta_\pi=120°$ and ≈ 0.3 for $\theta_\pi=64°$.

It is intriguing that, where there is a significant difference between data and DWIA, at the $\Delta(1232)$ the data are smaller than the DWIA calculation while at the N^* the data can be larger than the DWIA calculation.

It is not surprising that the N^*-nucleus interaction would be different from the $\Delta(1232)$-nucleus interaction. There are three main differences between the resonances: (1) the $\Delta(1232)$ has isospin $\frac{3}{2}$ while the N^*s have isospin $\frac{1}{2}$; (2) in the SU(6) representation, the quark wave function of the $\Delta(1232)$ has orbital angular momentum $L=0$, while the quark wave functions of the $S_{11}(1535)$ and the $D_{13}(1520)$ have $L=1$ [29]; and (3) the $\Delta(1232)$ form factor drops much more rapidly with momentum transfer than the proton or N^* form factors, indicating that the $\Delta(1232)$ is significantly larger than those baryons [30].

These measurements should be pursued in a more systematic way. One should make a measurement spanning a range of initial momenta at a variety of N^* momenta to determine whether the differences between data and DWIA is due to the large neutron initial momentum involved, i.e., due to a failure of the impulse approximation, or due to the smaller N^* momentum involved, i.e., due to the N^*-nucleus interaction. One should also measure the reaction at different pion angles to see whether the difference between the forward and backward angle results as observed at the $\Delta(1232)$ persists for the N^* and whether the difference is due to pion angle or to some other kinematic variable (e.g. to resonance momentum in the nucleus). Having isolated the various kinematic dependences of the reaction, one can then measure $(\gamma,\pi^- p)$ at a range of invariant masses to determine the interactions of the different resonances in the nuclear medium. This program would be well suited for large acceptance detectors at high duty factor facilities. Measurements of this nature will help elucidate the effects of baryon structure on the baryon-baryon interaction.

ACKNOWLEDGMENTS

The authors thank Shalev Gilad and Gerard van der Steenhoven for helpful discussions. The authors also thank the U.S. Department of Energy and the National Science Foundation for their generous support of this research.

[1] E. J. Moniz, in *Excited Baryons 1988,* edited by G. Adams, N. Mukhopadhyay, and P. Stoler (World Scientific, Singapore, 1988).
[2] G. S. Kyle *et al.*, Phys. Rev. Lett. **52**, 974 (1984).
[3] J. H. Koch and E. J. Moniz, Phys. Rev. C **27**, 751 (1983).
[4] D. Tieger *et al.*, Phys. Rev. Lett. **53**, 755 (1984).
[5] G. Girija *et al.*, Phys. Rev. C **27**, 1169 (1983).
[6] K. I. Blomqvist, "MEPS Design Report," Bates Internal Report (unpublished).
[7] R. S. Turley, Ph.D. thesis, MIT, 1984 (unpublished).
[8] L. B. Weinstein *et al.*, Phys. Rev. Lett. **64**, 1646 (1990).
[9] J. Morrison *et al.* (unpublished).
[10] G. van der Steenhoven *et al.*, Nucl. Phys. **A480**, 547 (1988).
[11] P. Stoler *et al.*, Phys. Rev. C **22**, 911 (1980).
[12] Ch. Schmitt *et al.*, Nucl. Phys. **A392**, 345 (1983).
[13] L. E. Wright and L. Tiator, Phys. Rev. C **26**, 2349 (1982).
[14] L. Tiator and L. E. Wright, Nucl. Phys. **A379**, 407 (1982).
[15] N. S. Chant and P. G. Roos, Phys. Rev. C **38**, 787 (1988); **39**, 957 (1989).
[16] J. M. Laget, Nucl. Phys. **A194**, 81 (1972).
[17] I. Arai and H. Fujii, Nucl. Phys. **B194**, 251 (1982).
[18] G. van der Steenhoven, private communication.
[19] A. Nadasen *et al.*, Phys. Rev. C **23**, 1023 (1981).
[20] W. B. Cottingame and D. B. Holtkamp, Phys. Rev. Lett. **45**, 1828 (1980).
[21] L. R. B. Elton and A. Swift, Nucl. Phys. **A94**, 52 (1967).
[22] L. B. Weinstein, Ph.D. thesis, MIT, 1988 (unpublished).
[23] L. D. Pham *et al.*, Phys. Rev. C **46**, 621 (1992); L. D. Pham, Ph.D. thesis, MIT, 1989 (unpublished).
[24] E. L. Lomon, private communication.
[25] P. S. Anan'in and I. V. Glavanakov, Yad. Fiz. **52**, 323 (1990) [Sov. J. Nucl. Phys. **52**, 205 (1990)].
[26] I. V. Glavanakov and V. N. Stibunov, Yad. Fiz. **29**, 1455 (1979) [Sov. J. Nucl. Phys. **29**, 746 (1979)].
[27] I. V. Glavanakov, Yad. Fiz. **49**, 91 (1989) [Sov. J. Nucl. Phys. **49**, 58 (1989)].
[28] G. van der Steenhoven, in Proceedings of the 7th Amsterdam Miniconference, 1991, edited by H. P. Blok, J. H. Koch, and H. de Vries (NIKHEF, Amsterdam, 1992).
[29] R. K. Bhaduri, *Models of the Nucleon* (Addison-Wesley, Redwood City, CA, 1988), pp. 30–43.
[30] P. Stoler, Phys. Rev. D **44**, 73 (1991).